

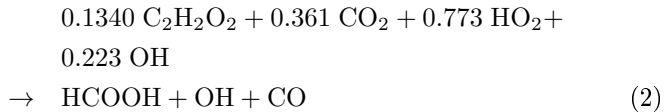
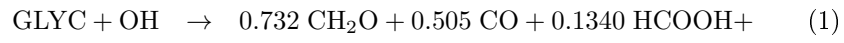
This is a supplement to the paper:

Importance of secondary sources in the atmospheric budgets of formic and acetic acids

by F. Paulot, D. Wunch, J. D. Crounse, G. C. Toon, D. B. Millet, P. F. DeCarlo, G. González Abad, J. Notholt, T. Warneke, C. Vigouroux, N. Deutscher, J. W. Hannigan, C. Warneke, J. A. de Gouw, E. J. Dunlea, M. De Mazière, D. W. T. Griffith, J. L. Jimenez, P. Bernath, P. O. Wennberg

Yield of formic and acetic acids from the from the oxidation of glycolaldehyde and hydroxyacetone by OH

FA is formed from the photooxidation of glycolaldehyde (Butkovskaya et al., 2006a). The yield of FA decreases while the yield of CH₂O increases as temperature increases. This is likely related to the channel CO + HCOOH + OH (2) since the increased production of FA is accompanied by an increased production of OH. To simplify the representation of this reaction, we divide the oxidation of glycolaldehyde by OH into two different pathways



The branching ratio between the pathways (1) and (2) is calculated using the measured yield of CH₂O and HCOOH at different temperatures : $Y_1 = 1 - 5.01 \times 10^{-6} \times \exp(\frac{2612}{T})$.

FA and AA are also formed in the photooxidation of hydroxyacetone (Butkovskaya et al., 2006b). The yields of FA and AA are obtained by assuming $Y_{\text{FA}} = Y_{\text{AA}}$ and $Y_{\text{FA}} + Y_{\text{AA}} + Y_{\text{C}_3\text{H}_4\text{O}_2} = 1$ which yields $Y_{\text{FA}} + Y_{\text{AA}} = 2.63 \times 10^{-3} \times \exp(1206/T)$.

Retrieval of FA by ground FTS

Method

For all stations but Thule and La Réunion, FA is retrieved from spectra using GFIT (Wunch et al., 2010). For Thule (Hannigan et al., 2009) and La Réunion (Senten et al., 2008), FA is retrieved using SFIT2 (Rinsland et al., 1998). Both retrieval method consist of a “forward model”, which computes an atmospheric transmittance spectrum for a prescribed set of conditions, and an “inverse method” which compares each measured spectrum with the calculation, and decides how best to modify the a priori profile to achieve a better match. GFIT scales the a priori profile via a non-linear least-squares spectral fitting algorithm. SFIT2 enables to retrieve a vertical profile by the use of the optimal estimation method (Rodgers, 2000). However, in the case of FA, the degree of freedom of the signal is very close to one, so that no additional independent piece of information can be obtained besides the total column, as for GFIT.

The a priori altitude, pressure, temperature and specific humidity profiles used in GFIT and SFIT2 are from NCEP/NCAR analysis product (Kalnay et al., 1996) with the exception of the cruises in the Atlantic ocean. The window used to retrieve FA is centered at 1106.32 cm^{-1} with a width of 6.75 cm^{-1} . For La Réunion, a smaller window ($1102.75 - 1106.4\text{ cm}^{-1}$) is used to avoid the strong water band at 1106.7 cm^{-1} .

Interfering gases are H_2O , O_3 , HDO, CH_4 , NH_3 , CCl_2F_2 and CHClF_2 (+ H_2^{18}O , H_2^{17}O , $^{16}\text{O}^{16}\text{O}^{18}\text{O}$ for La Réunion). For La Réunion, the profile of H_2O , O_3 , HDO, CCl_2F_2 and CHClF_2 is first retrieved using dedicated windows for each target molecule. Their profiles are then used to retrieve FA.

The FA retrieval is especially sensitive to the H_2O and O_3 profiles. We find that small modifications of the water spectroscopy in the FA window reduces the residuals. These modifications are :

- increase in the pressure shift from -0.0175 to $-0.0210\text{ cm}^{-1}/\text{atm}$
- increase in the width from 0.061 to $0.062\text{ cm}^{-1}/\text{atm}$
- increase in the temperature dependence of the width from 0.29 to 0.45 .

These modifications were applied in the retrieval at Barcroft, Bremen, Paramaribo and Wollongong as well as for the cruises.

For the cruises, we use measured H_2O and O_3 vertical profiles over the ship by balloon-borne radio and ozone sonde.

For Paramaribo, the O_3 profile is inferred from Shadoz measurements at the Paramaribo station (Thompson et al., 2003) combined with an ACE-FTS climatology.

For Thule, H_2O is retrieved by scaling H_2O a priori profile. O_3 and HCOOH are retrieved simultaneously.

For Wollongong, O_3 profiles are derived from monthly mean HALOE data (Russell et al., 1993).

Error Analysis

Error in the spectroscopy

The FA Q branch line intensity has an uncertainty of $\sim 7\%$ (Vander Auwera et al., 2007) which translates into a $\sim 7\%$ error in the retrieved FA total column. Fig. S1 illustrates the dependence of the retrieved FA at Paramaribo on the window used to retrieve FA (Table S1). The choice of the window used to retrieve FA could result in a systematic bias in the FA total column as large as $\sim \pm 2.7 \times 10^{15}$ molec/cm 2 .

Error in FA profile

Fig. S2 illustrates the effect of the a priori FA vertical profile (Fig. S3) on the retrieved FA total column at Paramaribo. FA retrieval at Barcroft, Bremen, Paramaribo and Wollongong as well as the Atlantic cruises use the FA vertical profile from the ATMOS mission as a priori. This profile assumes most FA is located in the boundary layer, i.e., that FA total column is driven by local sources. In contrast, the FA a priori vertical profile used in La Réunion (from PEM-tropics A (Hoell et al., 1999) and ACE-FTS (González Abad et al., 2009)) assumes that most FA peaks in the free troposphere, i.e., that FA total column is driven by transport. At Paramaribo, the modeled FA vertical profile shows evidence of both transport and local sources. The choice of a priori profile results in an uncertainty of $\sim 17\%$ in the retrieved FA profile.

The overall uncertainty is thus $\sim 19\%$ with a systematic bias up to $\pm 2.7 \times 10^{15}$ molec/cm 2 .

Tab. S1: Windows used to retrieve FA

	Center (cm^{-1})	Width (cm^{-1})	Interfering Chemical Species
P	1090.00	13.00	$\text{O}_3 \text{H}_2\text{O}$ HDO CCl_2F_2 CHClF_2 CH_4 NH_3 CO_2 CH_3OH CCl_3F
P_{s}	1091.50	10.50	$\text{O}_3 \text{H}_2\text{O}$ HDO CCl_2F_2 CHClF_2 CH_4 NH_3 CO_2 CH_3OH CCl_3F
Q	1106.32	6.75	$\text{O}_3 \text{H}_2\text{O}$ HDO CCl_2F_2 CHClF_2 CH_4 NH_3
Q_{s}	1104.60	3.65	$\text{O}_3 \text{H}_2\text{O}$ HDO CCl_2F_2 CHClF_2 CH_4 NH_3
R	1221.00	12.00	$\text{O}_3 \text{H}_2\text{O}$ HDO CCl_2F_2 CHClF_2 CH_4 NH_3 N_2O
R_{s}	1119.00	8.00	$\text{O}_3 \text{H}_2\text{O}$ HDO CCl_2F_2 CHClF_2 CH_4 NH_3 N_2O

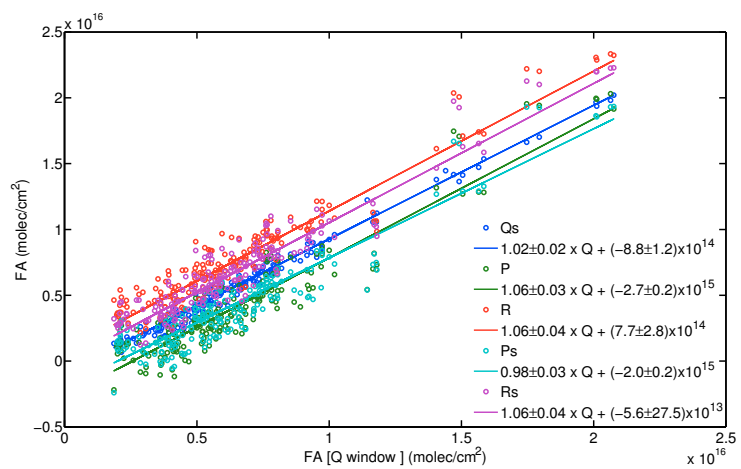


Fig. S1: Influence of the window on the retrieved FA total column at Paramaribo.

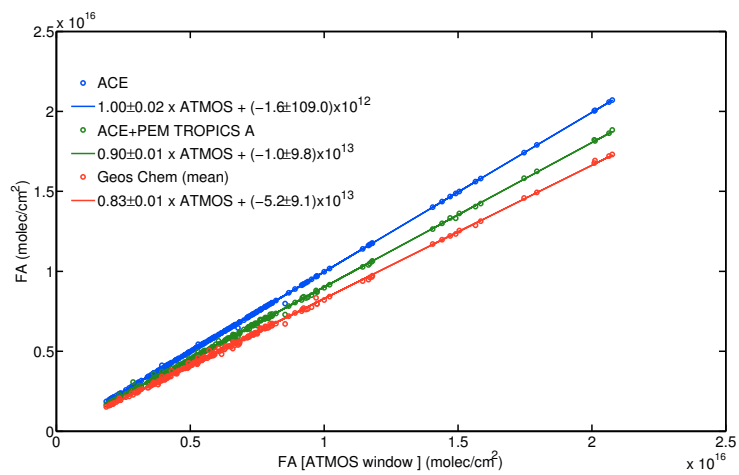


Fig. S2: Influence of FA a priori vertical profile on the retrieved FA total column at Paramaribo

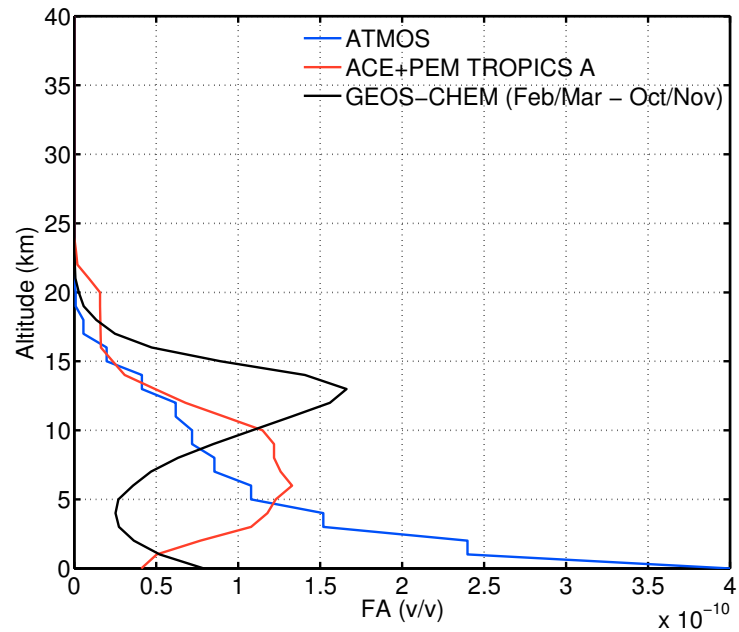


Fig. S3: A priori vertical profiles of FA used to retrieve FA total column.

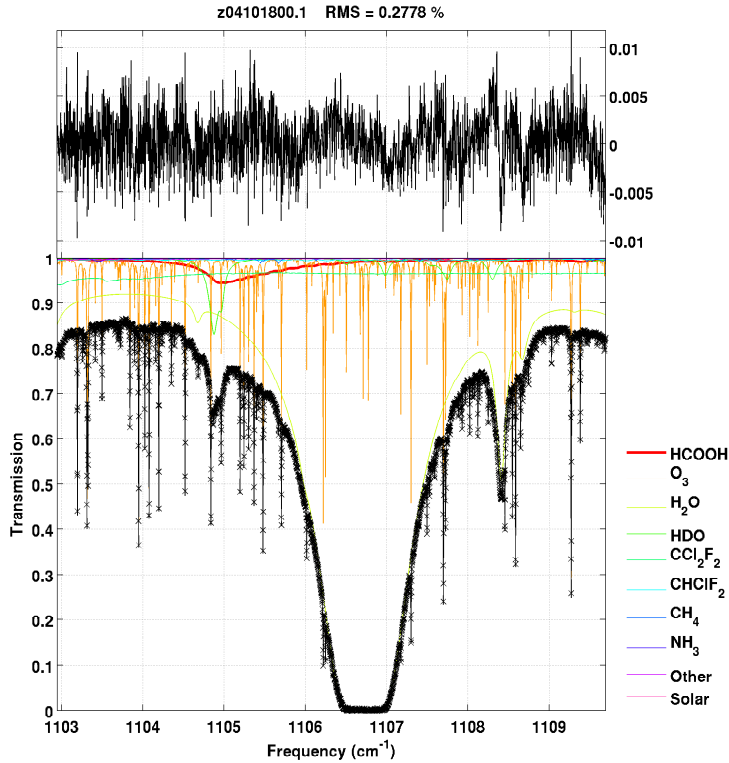


Fig. S4: An example of FA retrieval at Paramaribo using GFIT using the Q window. Top panel represent the fit residuals (computed - measured spectrum). Bottom panel represents the computed spectrum (black line), measured spectrum (black crosses) as well as the contribution of the different gases in the window used to retrieve FA. The weakness of FA absorption and the strong interference of H_2O in the region make the retrieval of FA challenging. For this spectrum, the retrieved FA total column is 1.02×10^{16} molec/cm².

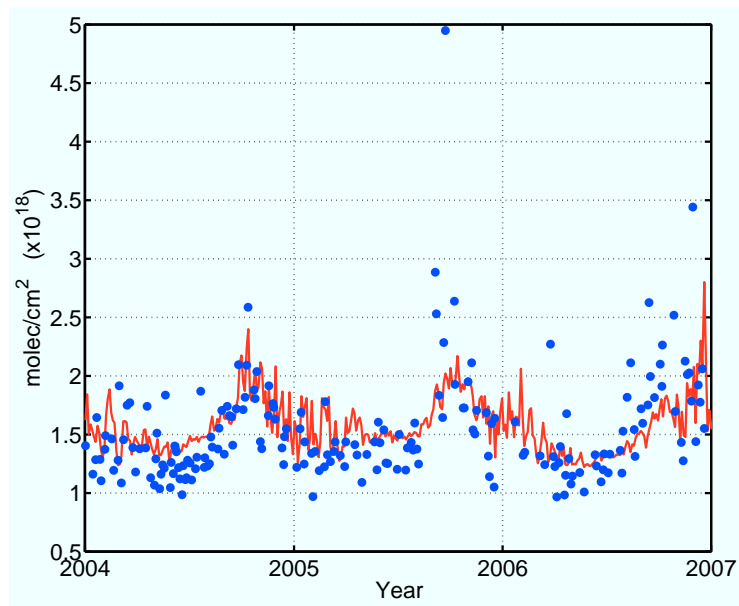


Fig. S5: Same as Fig. 3a for CO (Wollongong). Note the anomalously high CO at the end of 2007, reflecting intense biomass burning in the region.

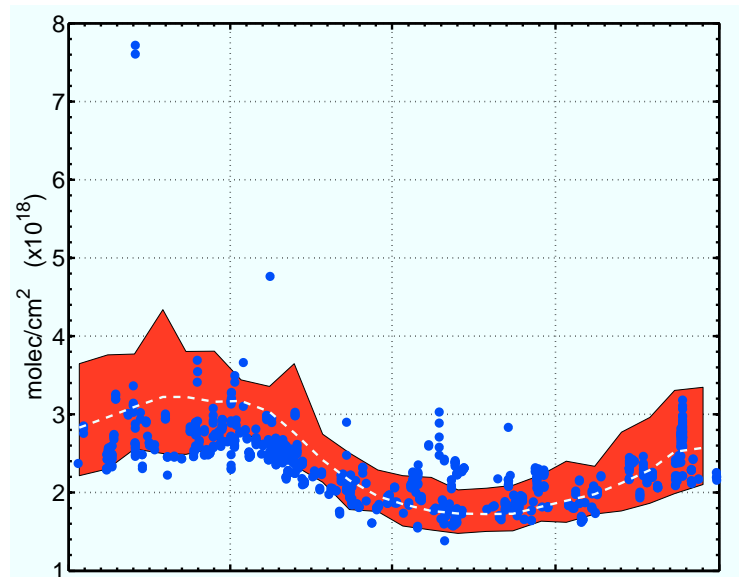


Fig. S6: Same as Fig. 4 for CO at Bremen

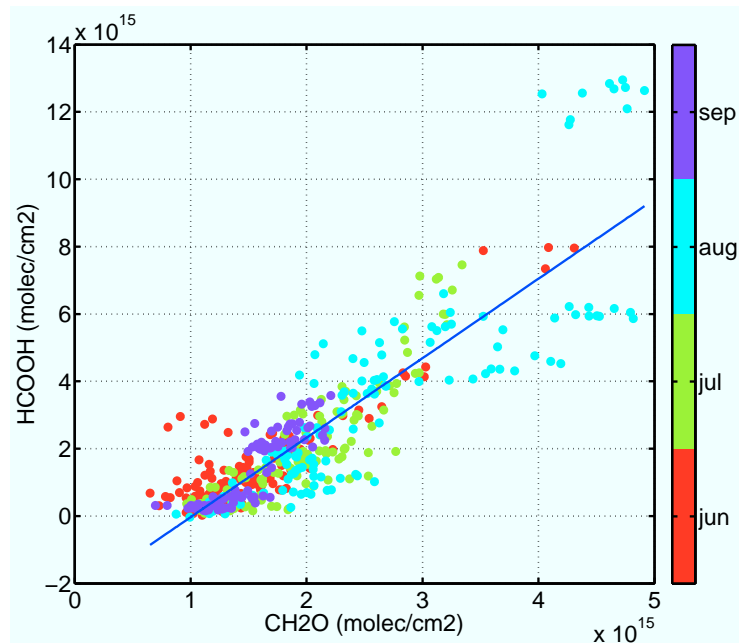


Fig. S7: Relationship between FA and CH₂O at Barcroft ($FA \simeq 2.3 \times CH_2O$, $R^2 = 0.77$)

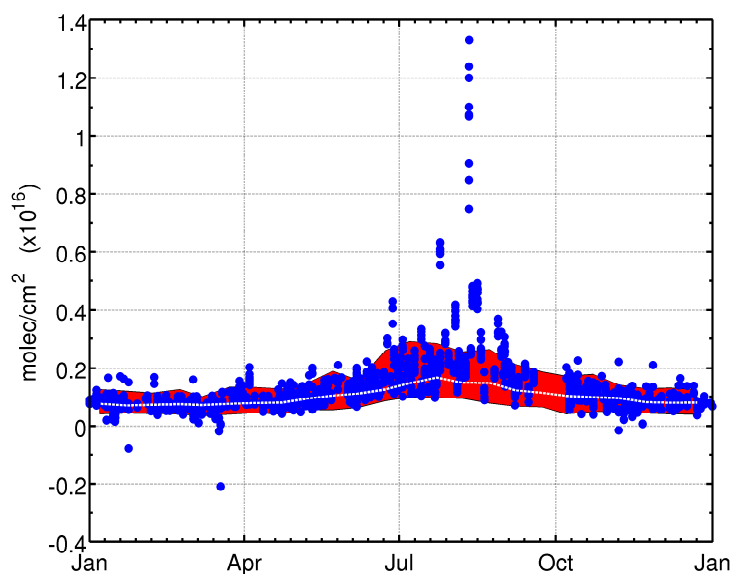


Fig. S8: Same as Fig. 4 for CH_2O at Barcroft

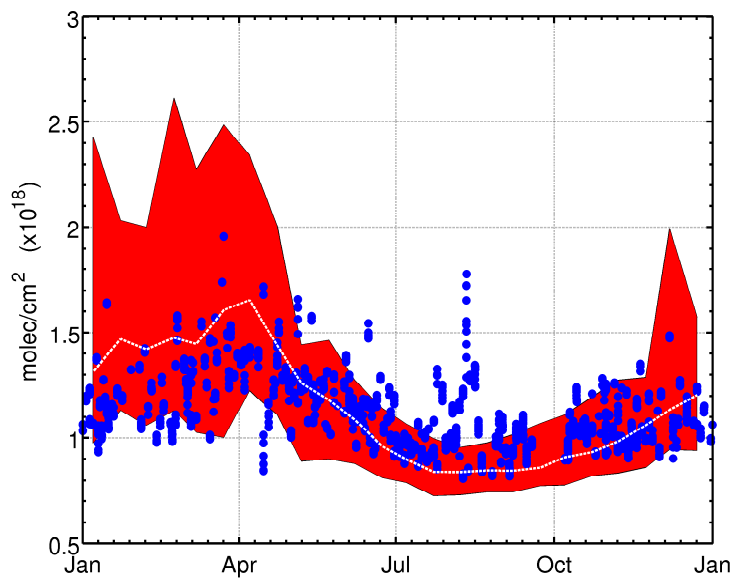


Fig. S9: Same as Fig. 4 for CO at Barcroft

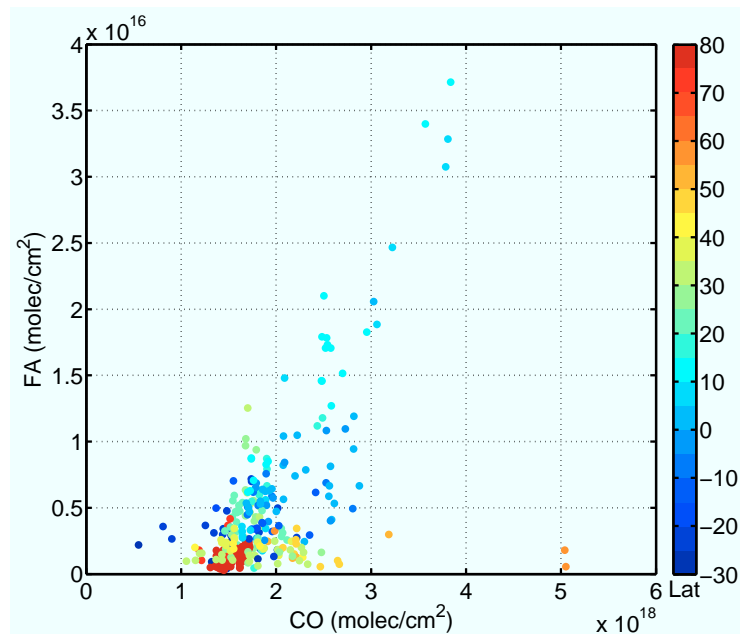


Fig. S10: Relationship between CO and FA total columns (molec/cm²) measured during cruises in the Atlantic Ocean.

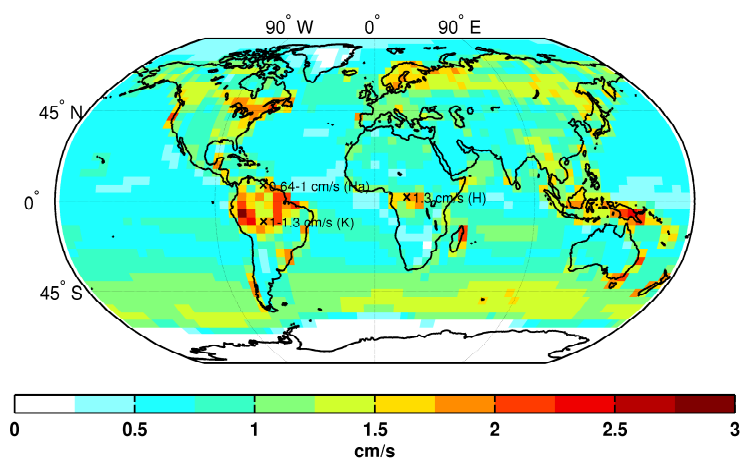


Fig. S11: Averaged modeled deposition velocity of FA from June to August. Crosses indicate deposition velocity measurements. Ha: Hartmann et al. (1991), H: Helas et al. (1992), K: Kuhn et al. (2002).

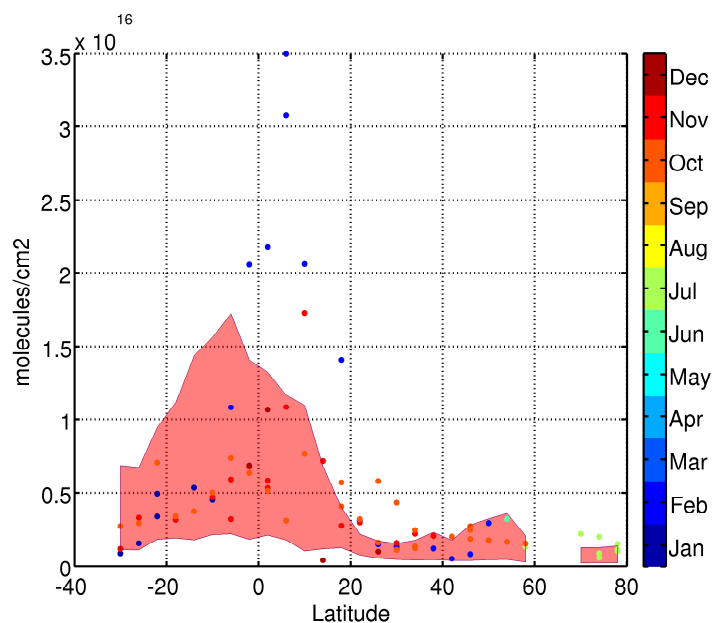


Fig. S12: Effect of a diffuse source of FA associated with aerosol aging on FA total column over the Atlantic (scenario R3). Color code same as Fig. 5.

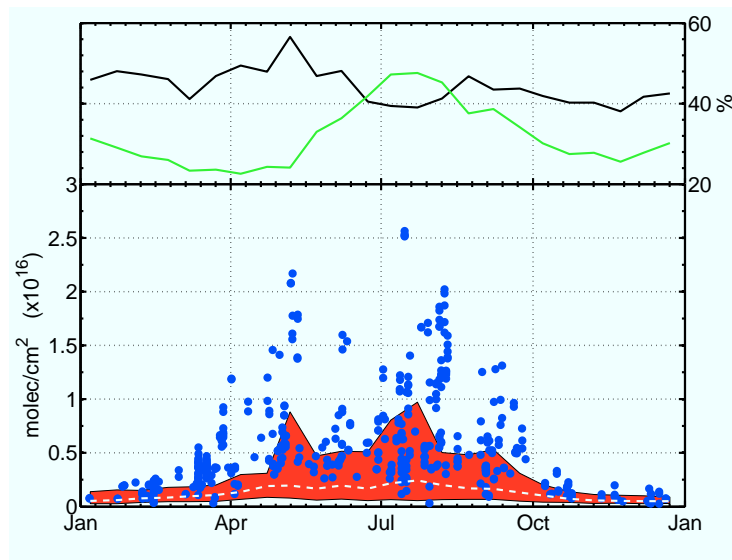


Fig. S13: Same as Fig. S10 for Bremen. Color code same as Fig. 4b.

Tab. S2: Regional and Global Burden for FA (in %)

	Tropics (24°S – 24°N)	Mid latitudes (76°S – 24°S)	(24°N – 76°N)	(90°S – 76°S)	Polar regions (76°N – 90°N)	Global
Biomass burning	1.4	0.7	1.3	0.6	1.2	1.2
Biofuel	0.2	0.1	0.5	0.0	0.4	0.2
Terrestrial vegetation	2.6	2.4	2.4	1.4	1.3	2.4
Soil	2.0	1.1	3.3	0.8	0.9	2.0
Anthropogenic (Fossil fuel + Cattle)	0.6	0.3	7.0	0.1	3.7	1.7
Photooxidation (biogenic)	82.5	82.7	64.2	76.2	55.5	79.2
Photooxidation (Anthropogenic +Biomass)	10.7	12.7	21.3	20.9	37.0	13.3
Overall	58.9	22.4	17.8	0.4	0.5	10.7 Gmol

Tab. S3: Regional and Global Burden for AA (in %)

	Tropics (24°S – 24°N)	Mid latitudes (76°S – 24°S)	Mid latitudes (76°N – 24°N)	Polar regions (90°S – 76°S)	Polar regions (76°N – 90°N)	Global
Biomass burning	12.3	6.0	8.2	3.7	6.7	10.2
Biofuel	3.6	1.5	12.1	0.7	9.7	4.7
Terrestrial vegetation	2.4	2.4	2.2	1.0	1.1	2.4
Soil	2.6	1.4	2.6	0.7	0.7	2.3
Anthropogenic (Fossil fuel + Cattle)	0.7	0.4	9.3	0.2	4.7	2.2
Photooxidation (biogenic)	77.2	86.5	64.2	91.1	74.4	76.9
Photooxidation (Anthropogenic +Biomass)	1.2	1.6	1.4	2.6	2.7	1.3
Overall	61.4	20.2	17.7	0.2	0.5	9.1 Gmol

References

- Butkovskaya, N. I., Pouvesle, N., Kukui, A., and Bras, G. L.: Mechanism of the OH-initiated oxidation of glycolaldehyde over the temperature range 233–296 K., *J. Phys. Chem. A*, 110, 13 492–13 499, doi:10.1021/jp064993k, 2006a.
- Butkovskaya, N. I., Pouvesle, N., Kukui, A., Mu, Y., and Le Bras, G.: Mechanism of the OH-initiated oxidation of hydroxyacetone over the temperature Range 236–298 K, *J. Phys. Chem. A*, 110, 6833–6843, doi:10.1021/jp056345r, 2006b.
- González Abad, G., Bernath, P. F., Boone, C. D., McLeod, S. D., Manney, G. L., and Toon, G. C.: Global distribution of upper tropospheric formic acid from the ACE-FTS, *Atmos. Chem. Phys.*, 9, 8039–8047, URL <http://www.atmos-chem-phys.net/9/8039/2009/>, 2009.
- Hannigan, J. W., Coffey, M. T., and Goldman, A.: Semiautonomous FTS Observation System for Remote Sensing of Stratospheric and Tropospheric Gases, *J. Atmos. Oceanic Technol.*, 26, 1814–1828, doi:10.1175/2009JTECHA1230.1, 2009.
- Hartmann, W. R., Santana, M., Hermoso, M., Andreae, M. O., and Sanhueza, E.: Diurnal cycles of formic and acetic acids in the northern part of the Guayana Shield, Venezuela, *J. Atmos. Chem.*, 13, 63–72, 1991.
- Helas, G., Bingemer, H., and Andreae, M. O.: Organic Acids Over Equatorial Africa: Results from DECAFE 88, *J. Geophys. Res.*, 97, 6187–6193, doi:10.1029/91JD01438, 1992.
- Hoell, J. M., Davis, D. D., Jacob, D. J., Rodgers, M. O., Newell, R. E., Fuelberg, H. E., McNeal, R. J., Raper, J. L., and Bendura, R. J.: Pacific Exploratory Mission in the tropical Pacific: PEM-Tropics A, August–September 1996, *J. Geophys. Res.*, 104, 5567–5584, doi:10.1029/1998JD100074, 1999.
- Kalnay, E., Kanamitsu, M., Kistler, R., Collins, W., Deaven, D., Gandin, L., Iredell, M., Saha, S., White, G., Woollen, J., et al.: The NCEP/NCAR 40-Year Reanalysis Project, *Bull. Am. Meteorol. Soc.*, 77, 437–471, 1996.
- Kuhn, U., Rottenberger, S., Biesenthal, T., Ammann, C., Wolf, A., Schebeske, G., Oliva, S., Tavares, T. M., and Kesselmeier, J.: Exchange of short-chain monocarboxylic acids by vegetation at a remote tropical forest site in Amazonia, *J. Geophys. Res.*, 107, 8069, doi:10.1029/2000JD000303, 2002.
- Rinsland, C. P., Jones, N. B., Connor, B. J., Logan, J. A., Pougatchev, N. S., Goldman, A., Murcray, F. J., Stephen, T. M., Pine, A. S., Zander, R., Mahieu, E., and Demoulin, P.: Northern and southern hemisphere ground-based infrared spectroscopic measurements of tropospheric carbon monoxide and ethane, *J. Geophys. Res.*, 103, 28 197–28 218, doi:10.1029/98JD02515, 1998.

-
- Rodgers, C.: Inverse methods for atmospheric sounding: Theory and practice, vol. 2 of *Atmospheric, Ocean and Planetary Physics*, World Scientific Singapore, 2000.
- Russell, III, J. M., Gordley, L. L., Park, J. H., Drayson, S. R., Hesketh, W. D., Cicerone, R. J., Tuck, A. F., Frederick, J. E., Harries, J. E., and Crutzen, P. J.: The Halogen Occultation Experiment, *J. Geophys. Res.*, 98, 10 777–10 797, doi:10.1029/93JD00799, 1993.
- Senten, C., De Mazière, M., Dils, B., Hermans, C., Kruglanski, M., Neefs, E., Scolas, F., Vandaele, A. C., Vanhaelewijn, G., Vigouroux, C., Carleer, M., Coheur, P. F., Fally, S., Barret, B., Baray, J. L., Delmas, R., Leveau, J., Metzger, J. M., Mahieu, E., Boone, C., Walker, K. A., Bernath, P. F., and Strong, K.: Technical Note: New ground-based FTIR measurements at Ile de La Réunion: observations, error analysis, and comparisons with independent data, *Atmos. Chem. Phys.*, 8, 3483–3508, doi:10.5194/acp-8-3483-2008, URL <http://www.atmos-chem-phys.net/8/3483/2008/>, 2008.
- Thompson, A., Witte, J., McPeters, R., Oltmans, S., Schmidlin, F., Logan, J., Fujiwara, M., Kirchhoff, V., Posny, F., Coetzee, G., et al.: Southern Hemisphere Additional Ozonesondes (SHADOZ) 1998–2000 tropical ozone climatology: 1. Comparison with Total Ozone Mapping Spectrometer (TOMS) and ground-based measurements, *J. Geophys. Res.*, 108, 8238, doi:10.1029/2001JD000967, 2003.
- Vander Auwera, J., Didriche, K., Perrin, A., and Keller, F.: Absolute line intensities for formic acid and dissociation constant of the dimer, *J. Chem. Phys.*, 126, 124 311–124 320, doi:10.1063/1.2712439, 2007.
- Wunch, D., Toon, G. C., Blavier, J.-F. L., Washenfelder, R., Notholt, J., Connor, B. J., Griffith, D. W. T., Sherlock, V., and Wennberg, P. O.: The Total Carbon Column Observing Network (TCCON), *Philos. Trans. R. Soc. London, Ser. A*, Accepted, 2010.